ISPC-8 Tokyo, 1987
Paper number BV-03

FLUID DYNAMIC CONTROL OF A PLASMA ENERGY FLOW BY A BLOWING GAS

T. Watanabe, T. Honda and A. Kanzawa

Department of Chemical Engineering
Tokyo Institute of Technology
Meguro-ku, Tokyo 152, JAPAN

ABSTRACT

Fluid dynamic control of plasma energy flow density was investigated numerically and experimentally. The enthalpy flow distributions of a thermal argon plasma jet were sharpened by an inward radially blowing gas. The blowing gas was injected from the circumference around the jet nozzle exit. The sharpness of the enthalpy flow distribution is dependent on the flow rate of the blowing gas.

1. INTRODUCTION

The control of the energy flow density of a plasma flow is required when the plasma flow is used for material treatments. For this purpose, hydrodynamic, magnetic or mechanical control may be available.

The object of this study is to sharpen the enthalpy flow distribution of a thermal plasma jet. In order to suppress the outward flow in the plasma jet, an inward radially blowing gas was injected from a circumferential slit around the jet nozzle exit.

The solutions of the set of the conservation equations have been reported for analytical models of a free-burning arc and a jet[1)-3)]. In this report, the velocity and the temperature fields of an argon plasma jet affected by the radially blowing gas were obtained numerically and experimentally, and then the effect of the blowing gas on the sharpness of the enthalpy flow distribution were investigated.

2. NUMERICAL ANALYSIS

2-1 Conservation Equations

In the numerical analysis, the following assumptions are employed: (1) steady state; (2) laminar flow; (3) axial symmetry; (4) single temperature; (5) body force and the radiation loss are neglected. Based on these assumptions, the conservation equations using cylindrical coordinate are expressed as follows:

(a) conservation of mass

$$\frac{\partial}{\partial z}(\rho u) + \frac{1}{r}\frac{\partial}{\partial r}(\rho r u) = 0 \tag{1}$$

where u and v are the axial and radial components of the plasma velocity, ρ is the plasma density, and z and r are the axial and radial coordinates, respectively.

(b) conservation of momentum

$$\rho\frac{\partial u}{\partial t} + \rho u\frac{\partial u}{\partial z} + \rho v\frac{\partial u}{\partial r} = -\frac{\partial P}{\partial z} + 2\frac{\partial}{\partial z}(\mu\frac{\partial u}{\partial z}) + \frac{1}{r}\frac{\partial}{\partial r}(\mu r\frac{\partial u}{\partial r}) + \frac{1}{r}\frac{\partial}{\partial r}(\mu r\frac{\partial v}{\partial z}) \tag{2}$$

$$\rho\frac{\partial v}{\partial t} + \rho u\frac{\partial v}{\partial z} + \rho v\frac{\partial v}{\partial r} = -\frac{\partial P}{\partial r} + \frac{\partial}{\partial z}(\mu\frac{\partial v}{\partial z}) + \frac{2}{r}\frac{\partial}{\partial r}(\mu r\frac{\partial v}{\partial r}) + \frac{\partial}{\partial z}(\mu\frac{\partial u}{\partial r}) - \frac{2\mu v}{r^2} \tag{3}$$

These equations include their time-dependent terms because of stability of the numerical solutions. In above equations, P is the pressure and μ is the viscosity.

(c) conservation of energy

$$\rho\frac{\partial h}{\partial t} + \rho u\frac{\partial h}{\partial z} + \rho v\frac{\partial h}{\partial r} = \frac{\partial}{\partial z}(\frac{k}{Cp}\frac{\partial h}{\partial z}) + \frac{1}{r}\frac{\partial}{\partial r}(\frac{kr}{Cp}\frac{\partial h}{\partial r}) \tag{4}$$

where h is the enthalpy, Cp is the specific heat at constant pressure and k is the thermal conductivity. This equation also includes time-dependent term.

2-2 Numerical Method

A time-relaxation method and a finite difference method are used. To simplify the calculation, the stream function and the vorticity defined as follows are used,

$$u = \frac{1}{\rho r}\frac{\partial \psi}{\partial r}, \quad v = \frac{-1}{\rho r}\frac{\partial \psi}{\partial z} \tag{5}$$

$$\zeta = \frac{\partial v}{\partial z} + \frac{\partial u}{\partial r} \tag{6}$$

where ψ is the stream function and ζ is the vorticity. The vorticity transport equation is obtained from Eqs.(2), (3), (5) and (6) as follows.

$$\rho\frac{\partial \zeta}{\partial t} + \frac{1}{r}\frac{\partial \psi}{\partial r}\frac{\partial \zeta}{\partial z} - \frac{1}{r}\frac{\partial \psi}{\partial z}\frac{\partial \zeta}{\partial r} + \frac{1}{r^2}\frac{\partial \psi}{\partial z}\zeta = \mu\Delta\zeta - \frac{\mu}{r^2}\zeta \tag{7}$$

The velocity and the temperature fields are calculated from Eqs.(4)-(7). A grid system consisting of 40 axial nodes and 20 radial nodes is employed.

2-3 Boundary Conditions

The boundary conditions and the calculation domains are specified in Fig.1. The plasma gas leaves the nozzle of an 8 mm-i.d. The side boundary (F-G) is given at 10 mm from the centerline and the upper boundary (G-H) is given at 40 mm from the nozzle exit. The inward radially blowing gas is injected from C-D. The blowing radius (R_B) (A-C) and the blowing width (W_B) (C-D) are chosen arbitrarily. These are similar to the size of the experimental apparatus. Along the centerline (A-H), symmetry conditions are used. The temperature (T) and ψ at the nozzle exit (A-B) are taken from the experimental data. At the blowing gas exit (C-D), T is 300 K and the radial velocity distribution is uniform. At B-C and D-F, no-slip conditions are employed and T is given 300 K. At the boundary F-G and G-H, the differentiation of ζ is taken as zero and the second order differentiations of T and ψ are zero.

2-4 Calculated Results

The lines in Figs.2 and 3 show the calculated results of the

plasma velocity and the temperature distributions. The keys in the figures show the experimental results explained later.

Figures 4 and 5 show the effect of the inward radially blowing gas. Q-value, which is defined by the ratio of the maximum of enthalpy flow (ρuh) to the half-value width, is adopted to evaluate the sharpness of the plasma jet. Figure 4 shows the effect of the flow rate of the blowing gas (V_B). Q-value has the maximum with the radially blowing gas flow rate around 3 l/min for every blowing radius. There are few differences for the blowing radius, but the blowing width has a strong influence on Q-value as shown in Fig.5, indicating that the blowing gas flow rate of the maximum Q-value becomes larger as the blowing width is larger.

The streamlines and isotherms for different parameter of the blowing width are shown in Figs.6 (a)-(c). ψ^* is normalized stream function divided by ψ at the nozzle exit. High temperature regions are extended and streamlines are gathered by the inward radially blowing gas. From these results, the radially blowing gas is found to be effective to sharpen the plasma flow.

3. EXPERIMENTS

3-1 Plasma Generator

An argon plasma jet at atmospheric pressure was employed as a thermal plasma flow. The sectional diagram of the plasma generator is shown in Fig.7. The argon plasma is generated by an arc discharge between an 8 mm-i.d. copper nozzle anode and a 6 mm-diam. tungsten rod cathode. The applied electric power is 3.2 kW. The flow rate of the argon gas is 10 l/min.

3-2 Temperature Measurements

The plasma temperature field is determined by using a calorimetric method. A 0.8 mm-diam. copper sphere with Cu-Co. thermocouple was swept perpendicularly to the axis at some sections of the plasma jet. From the temperature rise of the sphere, the plasma temperature can be obtained.

3-3 Velocity Measurements

The plasma velocity field can be obtained by using a water-cooled Pitot-tube, which is connected to a water manometer.

3-4 Experimental Results

The experimental results for the plasma velocity and the temperature are shown as the keys in Figs.2 and 3 in the numerical analysis section. There are some differences between the calculated and the experimental results, and the following reasons are considered. First, the experimental errors are included especially for low temperature domain. Second, the model used in the calculation is not perfect. However, these results are considered to be useful for the investigation of the sharpness of the plasma jet, which is the main purpose of this report.

The radially blowing gas was injected toward the center of the plasma flow in the same manner as the numerical model shown in Fig.1. Figure 8 shows the effects of the blowing gas on Q-value. Q-value has the maximum with the blowing gas flow rate

around 3 l/min. This is the same result as mentioned in the numerical analysis section. From the observation of the plasma jet flame, the length was noticed to be extended by the blowing gas; i.e., the length with 3 l/min blowing gas was 21.8 mm and that without blowing gas was 15.5 mm. This observation means that the blowing gas is effective to sharpen the plasma enthalpy flow distributions.

4. DISCUSSIONS AND CONCLUSIONS

Theoretical calculations have been made for the plasma jet flow with the blowing gas. Q-value was noted to have the maximum with the flow rate of the inward radially blowing gas. The effect of the variation of the blowing width is much larger than that of the blowing radius. Similar results are also recognized for the experimental results.

The enthalpy flow distribution of the plasma jet decays outward, because the plasma flow has the outward radial flow. The inward radially blowing gas from the circumferential slit has much effect to suppress the outward radial flow, although the excess of the blowing gas works negatively because of the overcooling of the plasma flow.

REFERENCES

(1) J. McKelliget, J. Szekely, M. Vardelle and P. Fauchais; Plasma Chem. Plasma Process. 2, 317 (1982)

(2) K. C. Hsu, K. Etemadi and E. Pfender; J. Appl. Phys., 54, 1293 (1983)

(3) P. Kovitya and J. J. Lowke; J. Phys. D: Appl. Phys., 18, 53 (1985)

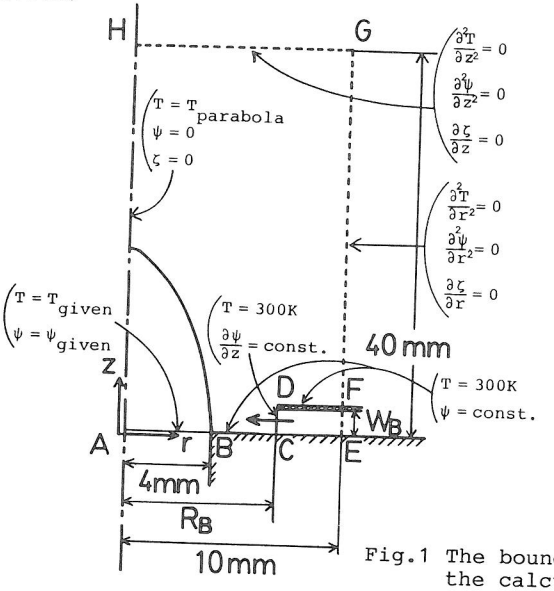

Fig.1 The boundary conditions and the calculation domains

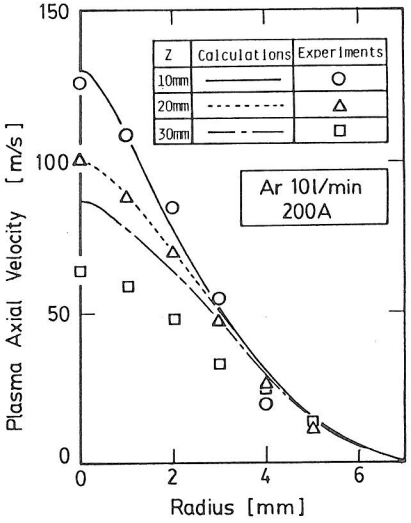

Fig.2 Plasma axial velocity distribution

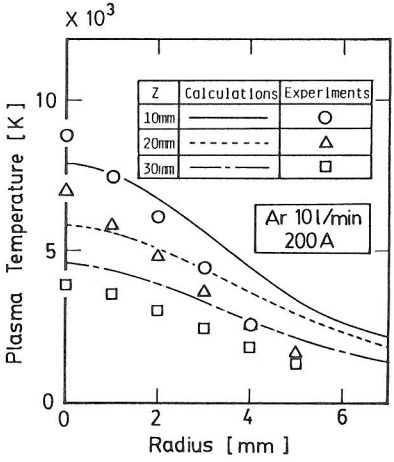

Fig.3 Plasma temperature distribution

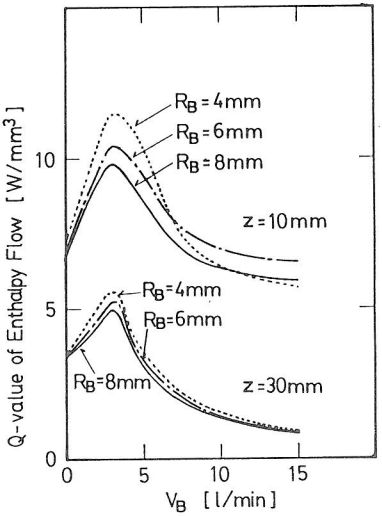

Fig.4 Calculated Q-value; W_B=1mm

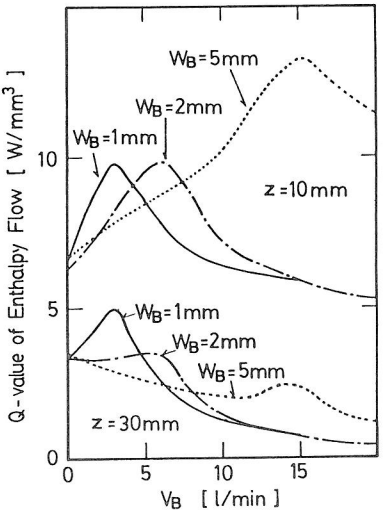

Fig.5 Calculated Q-value; R_B=8mm

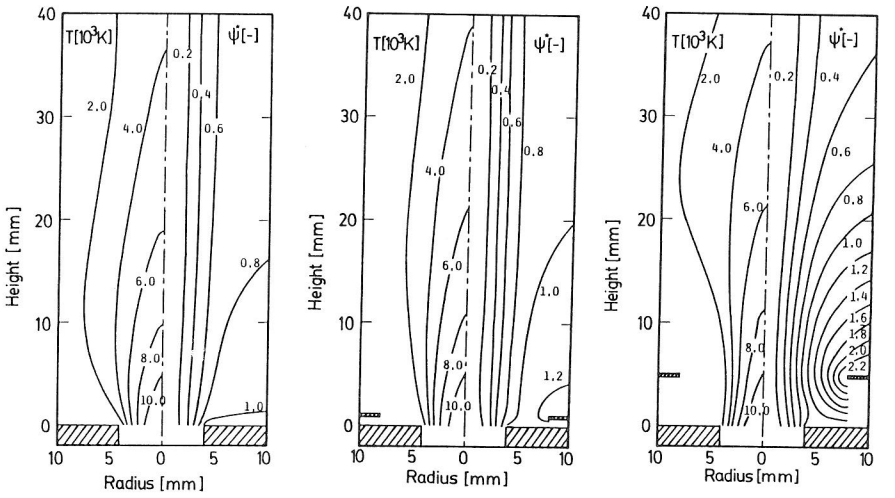

Fig.6 Calculated isotherms and streamlines; (a) no blowing gas; (b) W_B=1 mm, V_B=3 l/min; (c) W_B=5 mm, V_B 15=l/min

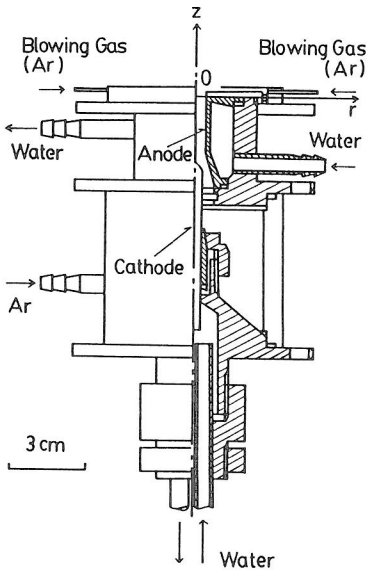

Fig.7 Plasma generator

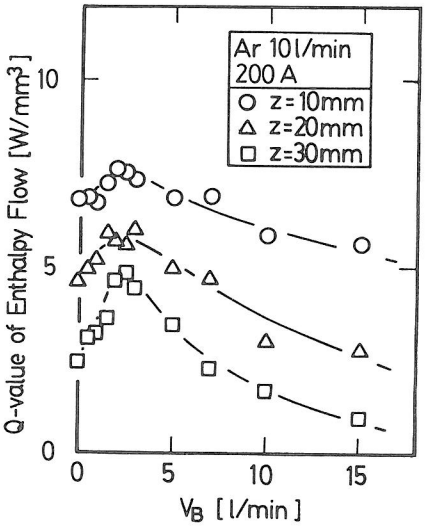

Fig.8 Measured Q-value; R_B=8mm, W_B=1mm